

Tunneling Spectroscopy of $\text{Tl}_2\text{Ba}_2\text{CuO}_6$

Lutfi Ozyuzer^{1,2,*}, Zikri Yusof^{1,3}, John F. Zasadzinski^{1,3},
Ting-Wei Li¹, Dave G. Hinks¹, and K. E. Gray¹

¹ *Science and Technology Center for Superconductivity and Materials Science Division,
Argonne National Laboratory, Argonne IL 60439*

² *Department of Physics, Izmir Institute of Technology, TR-35230 Izmir, Turkey*

³ *Science and Technology Center for Superconductivity,
Illinois Institute of Technology, Chicago, IL 60616*

New results from tunneling spectroscopies on near optimally-doped single crystals of $\text{Tl}_2\text{Ba}_2\text{CuO}_6$ (Tl-2201) junctions are presented. The superconductor-insulator-normal metal (SIN) tunnel junctions are obtained using the point-contact technique with a Au tip. The tunneling conductances reproducibly show a sharp cusp-like subgap, prominent quasiparticle peaks with a consistent asymmetry, and weakly decreasing backgrounds. A rigorous analysis of the SIN tunneling data is performed using two different models for the $d_{x^2-y^2}$ (*d*-wave) density of states (DOS). Based on these and earlier results, the tunneling DOS of Tl-2201 have exhibited the most reproducible data that are consistent with a *d*-wave gap symmetry. We show that the dip feature at 2Δ that is clearly seen in SIN tunneling data of $\text{Bi}_2\text{Sr}_2\text{CaCu}_2\text{O}_{8+\delta}$ is also present in Tl-2201, but at a weaker level. The gap values for crystals with a bulk $T_c = 86$ K are in the range of 19-25 meV.

PACS numbers: 74.50.+r, 74.80.Fp, 74.72.Fq

Keywords: High-temperature superconductivity, tunneling, superconducting gap.

I. INTRODUCTION

Tunneling spectroscopy has revealed the complex characteristics of high- T_c superconductors (HTS's). Tunneling spectra on $\text{Bi}_2\text{Sr}_2\text{CaCu}_2\text{O}_{8+\delta}$ (Bi-2212) [1,2], $\text{Bi}_2\text{Sr}_2\text{CuO}_x$ [3] and $\text{HgBa}_2\text{CuO}_4$ (Hg-1201) [4,5], have shown both symmetric and asymmetric tunneling conductance peaks, and variable subgap features that range from sharp cusp-like to flat, BCS-like. Additionally, tunneling experiments on $\text{YBa}_2\text{Cu}_3\text{O}_7$ (YBCO) and Bi-2212 in certain crystal orientations have also shown the presence of zero-bias peaks in the conductance data. [6-8] In Bi-2212 there exists a prominent dip feature (at $\text{eV} \sim 2\Delta$) that is asymmetric with bias voltage, being much stronger for a polarity that corresponds to removal of quasiparticles from the superconductor. These unusual observations have made it difficult to properly analyze the results of tunneling experiments and have complicated the deduction of important properties of HTS's such as the pairing symmetry.

There is an emerging consensus that the predominant pairing symmetry in hole-doped HTS cuprates is $d_{x^2-y^2}$ (*d*-wave). Evidence from tricrystal ring [9] experiments points to pure *d*-wave for YBCO. Grain boundary [10] and scanning tunneling microscopy (STM) [7] junctions indicate a small *s*-wave contribution to the *d*-wave symmetry on YBCO which was attributed to the orthorhombicity of YBCO. Tunneling [11] and penetration depth [12] measurements of electron-doped $\text{Nd}_{2-x}\text{Ce}_x\text{CuO}_4$ are compatible with *s*-wave symmetry. Another well-studied, hole doped, HTS is Bi-2212 because of the availability of high quality single crystals, and the ability to easily cleave this crystal along the *a*-*b* plane. Results from angle resolved photoemission spectroscopy (ARPES) indicate an anisotropic gap with a minimum in the (π, π) direction that is consistent with *d*-wave symmetry [13]. Furthermore, results from ARPES and STM have exhibited spectral features that are also observed in PCT, such as quasiparticle peak, dip and hump. They have also shown the puzzling feature of an increasing energy gap size with decreasing doping concentration in Bi-2212. [1,2] DeWilde et al. [1] have shown that the study on Bi-2212 using three different techniques (PCT, break-junction, and STM) can produce very similar results as far as gap size, dip structure, and subgap shape are concerned, even when the resistance of the STM junction was of the order of $\text{G}\Omega$ while it was the order of $1\text{k}\Omega$ - $100\text{k}\Omega$ for PCT and break junction. However, point contact tunneling (PCT) results also occasionally show a flat subgap structure [1] which is not easily reconciled with *d*-wave symmetry.

Quasiparticle tunneling has failed to definitely reveal the pairing symmetry in Hg-1201. PCT on polycrystal samples of this HTS seems to show a density of states (DOS) that is flat near zero-bias, consistent with *s*-wave symmetry

*Tel.: (630) 252 8457; Fax: (630) 252 7777; e-mail: ozyuzer@anl.gov

[4,14], whereas Wei *et al.* [5] claim that STM measurements on the same HTS seems to be consistent with a *d*-wave gap symmetry. While it has been shown that tunneling directionality effects can produce a flat subgap conductance with a *d*-wave gap, [15] there is no obvious physical mechanism for preferred tunneling directions. It is therefore more likely that the sporadic observations of flat subgap conductances in HTS simply adds fuel to the debate over pairing symmetry.

Experimental evidence of *d*-wave pairing symmetry on Tl-2201 is more convincing. Results from tricrystal ring experiments indicate a pure *d*-wave pairing [16], although admixture of *d* and *s*-wave pairing is also interpreted from in-plane torque anisotropy experiments. [17] We have earlier reported [18] the tunneling studies of optimally-doped $Tl_2Ba_2CuO_6$ crystals (Tl-2201) with $T_c = 91$ K which clearly and reproducibly showed a tunneling DOS that is consistent with a momentum-averaged *d*-wave gap symmetry. In that report (Ref. [18]), our analysis of the superconductor-insulator-normal metal (SIN) tunneling conductance was somewhat primitive, utilizing a simple model for the *d*-wave DOS. In this report, we present additional tunneling data on Tl-2201 crystals with $T_c = 86$ K that have been synthesized using a different technique than the one described in Ref. [18]. The location of the quasiparticle peaks in the SIN conductance data are consistent with the ones in our earlier report and all of the data again display the cusp feature at zero bias. However, here we present a more exhaustive treatment of many junctions, with a wide range of junction conductance (~ 0.1 mS-2 mS). We have also performed a more rigorous analysis of the SIN conductance data using two different models for the tunneling DOS with a *d*-wave gap. We again find good agreement with *d*-wave symmetry.

Some of the SIN data display a weak dip feature at $eV \sim 2\Delta$. We have generated superconductor-insulator-superconductor (SIS) conductance curves using the SIN data. The resulting SIS curves display the characteristic dip features at nearly 3Δ that are consistent with those observed in the SIS tunneling conductance of Bi-2212. This is the first study to clearly indicate that the dip feature is present in the SIN conductance data of Tl-2201, but with a smaller magnitude than observed in Bi-2212. Further comparison with tunneling data of Bi-2212 reveals that while the bulk T_c of Bi-2212 and Tl-2201 are approximately the same, the magnitude of the typical energy gap of Tl-2201 is smaller. The origin of this discrepancy is still unknown at present, but some insight has been gained with this study. We note first that the largest gaps found for the Tl-2201 ($\Delta = 25$ meV) are close to those of Bi-2212 when both have the same $T_c = 86$ K. Furthermore, due to the strong dependence of the gap magnitude on doping concentration [1] in Bi-2212, we suggest that the smaller gap values in Tl-2201 may be due to a surface that is slightly overdoped.

II. EXPERIMENTAL PROCEDURE AND RESULTS

Tl-2201 has a tetragonal crystal structure with a single $Cu - O$ layer per unit cell which is relatively simple when compared to the bilayer and trilayer high- T_c superconductors. However, $Tl_2Ba_2Ca_{2-n}Cu_2O_{2n+3}$ ($n=1, 2$, and 3) family is very sensitive to thallium and oxygen content which influences the structure and superconducting properties. [19] The optimally-doped compound of Tl-2201 has a T_c of approximately 91 K and this value can be reduced to zero on the overdoped side by oxygen annealing. [20]

The Tl-2201 single crystals were grown from a flux in an alumina crucible with an alumina lid, sealed to avoid loss of thallium oxide. Tl_2O_3 , BaO_2 and CuO powders were mixed at the atomic ratio of $Tl:Ba:Cu = 2.2:2:2$ using excess Tl_2O_3 and CuO as the flux. The crucibles, containing about 50 g of charge, were loaded in a vertical tube furnace and heated rapidly to 925-950°C. This temperature was held for 1/2 hour. The furnace was then cooled at 5 °C/h to 875°C, and finally cooled to room temperature. The crystals were platelet-shaped, with a basal plane area of about 1 mm² and a thickness along the *c*-axis varying between 20-100 μm. The critical temperature of the samples is determined by *ac* magnetization measurements.

The experimental setup of our PCT system is designed for data collection over a large range of sample temperature. In addition to this feature, tunneling measurements can also be performed in high magnetic fields, up to 6 T. The details of the measurement system can be found elsewhere. [21] Cleaved single crystal samples of Tl-2201 usually have shiny surfaces in the *a-b* plane. Each is mounted on a substrate using an epoxy so that the tip approaches nominally along the *c*-axis. The electrical leads are connected to two sides of the sample by using silver paint. Non-superconducting *Au* is used as a counter-electrode. It is mechanically and chemically cleaned before each run.

While the differential micrometer driven tip approaches the sample, the $I(V)$ signal is continuously monitored on an oscilloscope until an acceptable tunnel junction is obtained, i.e. one which displays an obvious superconducting gap feature. All tunnel junctions are initially formed at 4.2 K to prevent any sample surface deterioration. First derivative measurements, $\sigma = dI/dV$, were obtained using a Kelvin bridge circuit with the usual lock-in procedure. $I(V)$ and dI/dV are simultaneously plotted on a chart and digitally recorded on a computer. DeWilde *et al.* [1] have

shown that tunneling results on Bi-2212 using PCT can produce results that are consistent with those obtained using STM.

In contrast to other surface sensitive experimental methods such as STM, ARPES, Raman, and auger techniques, the advantage of the point contact method for cuprates is that the tip can be used to scrape, clean, and in some cases cleave the surface. The tip often can penetrate through the surface and reach the bulk of the crystal. The cleaving of the surface sometimes results in the formation of SIS junctions, as in the case of Bi-2212. This happens when a piece of the HTS crystal attaches itself to the tip, forming an ohmic contact. As the tip is retracted, the piece forms an SIS break junction with the bulk crystal [22]. Unlike Bi-2212, Tl-2201 has stronger bonds between planes and consequently SIS junctions could not be formed this way.

Figure 1 shows the conductances of eight junctions on three different Tl-2201 crystals, each with a bulk T_c near 86 K. These junctions are representative of a larger set of data and they demonstrate several characteristics that are typical for PCT tunneling in Tl-2201. Each junction exhibits a single energy gap feature with conductance peaks at $|V| = 20 - 25$ mV. The voltage is that of the sample respect to the tip and thus negative bias corresponds to removal of electrons from the superconductor. There is a characteristic asymmetry in the conductance peaks such that the negative bias peak is higher than the one at positive bias. This type of asymmetry has also been seen in PCT and STM studies of Bi-2212, most consistently in overdoped samples. It has been pointed out that this conductance peak asymmetry may be a signature of the d -wave pairing. [15]

The background conductances for $|eV| > \Delta$ are generally weakly decreasing with bias similar to that in Bi-2212, and it is these type of junctions that exhibit the largest peak height to background (PHB) ratio. A few junctions show a flat or slightly increasing background with a smaller PHB ratio. This implies that the decreasing background is an intrinsic property of the quasiparticle DOS. While such a feature may be due to the underlying band structure DOS, we note the absence of any van Hove singularity (VHS) in these data as well as earlier PCT data on Tl-2201. All of the junctions exhibit a cusp-like feature at zero bias which is characteristic of a d -wave DOS.

III. THEORETICAL MODEL

The tunneling data are analyzed with two different methods. For Model I, the superconducting data are first normalized by constructing a "normal state" conductance obtained by fitting the high bias data to a third order polynomial. The normalized conductance data are compared to a weighted momentum averaged d -wave DOS,

$$N(E) = \int f(\theta) \frac{E - i\Gamma}{\sqrt{(E - i\Gamma)^2 - \Delta(\theta)^2}} d\theta.$$

Here Γ is a lifetime broadening factor, $f(\theta)$, [23] is an angular weighting function, and $\Delta(\theta) = \Delta_o \cos(2\theta)$ represents the d -wave gap symmetry expected from a mean-field BCS-type interaction. [24] This model is used because it allows for a quick estimation of the gap value and as we will show, gives an excellent fit to the data. The inclusion of the weighting function allows for a better fit with the experimental data in the gap region than with the non-weighted average as was done previously. [18] Here, a weighting function $f(\theta) = 1 + 0.4\cos(4\theta)$ was used which imposes a preferential angular selection of the DOS along the absolute maximum of the d -wave gap and tapers off towards the nodes of the gap. This is a rather weak directional function since the minimum of $f(\theta)$ along the nodes of the d -wave gap is still non-negligible.

The second method (Model II) makes no attempt to normalize out any background conductance. Rather, an attempt is made to fit the entire spectrum by including a band structure, tunneling matrix element, and d -wave gap symmetry. [15] The tunneling DOS is calculated using the single particle Green's function,

$$N(E) = -\frac{1}{\pi} \text{Im} \sum_{\mathbf{k}} |T_{\mathbf{k}}|^2 G(\mathbf{k}, E) \quad (1)$$

For the superconducting state,

$$G(\mathbf{k}, E) = \frac{u_k^2}{E - E_k + i\Gamma} + \frac{v_k^2}{E + E_k + i\Gamma}$$

where u_k^2 and v_k^2 are the usual coherence factors, Γ is the quasiparticle lifetime broadening factor, and $E_k = \sqrt{|\Delta(\mathbf{k})|^2 + \xi_{\mathbf{k}}^2}$ with the gap function for d -wave symmetry $\Delta(\mathbf{k}) = \Delta_o[\cos(k_x a) - \cos(k_y a)]/2$. The tunneling matrix element $|T_{\mathbf{k}}|^2$ is written as

$$|T_{\mathbf{k}}|^2 = v_g D(\mathbf{k})$$

where v_g is the group velocity defined as $v_g = |\nabla_{\mathbf{k}} \xi_{\mathbf{k}} \cdot \mathbf{n}|$ and $D(\mathbf{k})$ is the directionality function that has the form [25]

$$D(\mathbf{k}) = \exp \left[-\frac{k^2 - (\mathbf{k} \cdot \mathbf{n})^2}{(\mathbf{k} \cdot \mathbf{n})^2 \theta_o^2} \right] \quad (2)$$

Here the unit vector \mathbf{n} defines the tunneling direction, which is perpendicular to the plane of the junction, whereas θ_o corresponds to the angular spread in k -space of the quasiparticle momenta with respect to \mathbf{n} that has a non-negligible tunneling probability.

The band structure for the $Cu - O$ plane extracted from ARPES measurements on Bi-2212 is used. [26] Presumably, other than the exact value of the chemical potential, the band structure for Tl-2201 [27] should have the same generic features as the extracted band structure from Bi-2212. Unlike a similar analysis done in our earlier report, [18] the presence of the VHS is not artificially removed by using a large chemical potential. Rather, the presence of the VHS is effectively diminished by the group velocity factor from the tunneling matrix element. [15,28] Here, the value of the chemical potential has been altered slightly to produce the best comparison to the experimental data. The tunneling DOS from this model is compared directly to the experimental conductance data using a constant scaling factor. An interesting aspect of this second model is the robust asymmetric quasiparticle peaks in the tunneling DOS. This asymmetry, which has the higher peak in the filled states, is a direct consequence of the d -wave gap symmetry and directionality in the model. As will be shown, this result is consistent with our experimental tunneling data.

IV. ANALYSIS AND DISCUSSION

Figures 2 and 3 present two representative SIN tunneling conductances of Tl-2201. Figure 2 shows Junction E of Fig. 1, while Figure 3 is an additional conductance curve (Junction J) not shown in Fig. 1 that has a very high peak height to background ratio. As illustrated in Figs. 2(a) and 3(a), the SIN conductance data consistently display the sharp, cusp-like subgap feature, weakly decreasing background, and conductance peaks that are either weakly or strongly asymmetric, with the higher peak on the negative bias side. The presence of these features and the overall shape of the conductance data are very similar to the conductance data of Fig. 1 in our earlier report. [18]

To compare the two data sets to Model I, the SIN conductance data are first normalized by dividing through with an extrapolated normal state conductance curve which is shown as the solid line in Fig. 2(a) and 3(a). [18] The normalized conductances are then compared to the DOS obtained from Model I as shown in Fig. 2(b) and 3(b). Other than a remaining conductance peak asymmetry and somewhat broader experimental peaks, the model DOS shows a remarkably good overall fit in the gap region with the experimental DOS. Notice that while the process of normalization has reduced the degree of asymmetry of the conductance peaks in both data sets, it has not eliminated it. This proves that the asymmetry is not a consequence of the background.

The comparison of Model II with the unnormalized tunneling data is shown in Fig. 2(c) and 3(c). The most striking observation is the model's ability to reproduce the peak asymmetry that is seen in the data. As was shown in Ref. [15], this type of asymmetry with the higher peak in the filled states is a robust property of d -wave gap symmetry and directional tunneling. The strength of the directionality here is defined by θ_o and the values used to compare both experimental data here are considerably larger than the ones used to analyze the Bi-2212 data. [15] This implies that these two data sets are best fit with a weak directional tunneling processes which is consistent with the type of weighting function $f(\theta)$ in Model I.

As in Bi-2212, Model II could not accurately reproduce the background conductance although it does show the generic decreasing background seen in both data sets. This may also be due to the fact that we are not using the exact normal state band structure for Tl-2201 in the model. Model II also produces a poorer agreement with the subgap data which might be due to the particular choice of directionality function used. Note that the values of the energy gap from both models are very close to each other, with the Model I having a slightly lower gap values than Model II.

We would like to point out that attempts at comparing the normalized experimental data with just a pure d -wave gap symmetry without the $f(\theta)$ weighting function in the Model I led to a poorer fit to the data. Considering this, we reanalyze some of the SIN tunneling data from our previous report (Junction B and C in Fig. 4 of Ref. [18] and relabeled here as Junction B' and C' respectively). We have restricted this analysis by using only Model I. Figure 4(a) shows the raw SIN conductance data of Junction B' and the estimated normal state conductance used to obtain the normalized data. This normalized curve is shown in Fig. 4(b) along with the comparison to Model I. The model

produces a better fit in the gap region (with identical gap value) when compared to our earlier fit. This procedure is repeated for Junction C' as shown in Fig. 4(c) (which has been normalized by a constant). In this case, the overall fit is only slightly improved over the one we reported earlier, with an identical gap value.

One of the distinct features of the tunneling DOS in Bi-2212 is the strong dip beyond the quasiparticle peak [29] in the occupied states. This feature is clearly seen in SIN conductance data of Bi-2212 from both STM and PCT. [1] Furthermore, this dip feature is enhanced in the superconductor-insulator-superconductor (SIS) junction. This is apparent from the break junction tunneling data in Ref. [1]. Our SIN conductance data of Tl-2201 from this work and in our previous report do not seem to distinctively show the same dip features, although there is evidence of a weak dip feature in the normalized data of Figs. 2 and 4 as well as junctions C and G in Fig. 1. We explore this issue further by generating SIS conductance curves from the raw data of Junction E and Junction B' which should enhance any dip feature that may exists in these SIN data. As shown in Fig. 5, both conductance data generate SIS curves that are qualitatively similar to the experimental SIS tunneling data of Bi-2212. [1] Both curves clearly display the prominent dip features located at slightly less than 3Δ . This indicates that the dip feature is also present in the SIN conductance data of Tl-2201 but at a smaller amplitude than the ones observed in the SIN data of Bi-2212.

Another significant difference between the tunneling data of Bi-2212 and Tl-2201 is the magnitude of the superconducting gap and this might be related to the dip feature discussed above. The optimally-doped Bi-2212 which has a T_c of 93-95 K has an energy gap in the range of 37-38 meV. [1] Due to the high reproducibility of the gap value for Bi-2212, it is presumed that the gap value for Bi-2212 is consistent with its T_c . Tl-2201 which has a bulk T_c of 86 K in this study and 91 K in the previous study, has an energy gap in the range of 19-25 meV. This value is considerably less than the energy gap of Bi-2212 even though bulk T_c for both cuprates are roughly the same. This discrepancy raises an important question in HTS cuprates, namely the relationship between gap size $\Delta(T = 0)$ and T_c . The unusual Δ versus doping in Bi-2212, which violates mean-field theory, strongly suggest that T_c is a phase coherence temperature. In this picture, there are strong superconducting fluctuations above T_c and presumably the ability of each HTS to support such fluctuations depends on structural parameters, anisotropy and the degree of 2-dimensionality. It is thus possible that there is no universal relationship between Δ and T_c for all HTS. If there exists a universal relationship between these two parameters for HTS cuprates as is approximately the case for conventional superconductors, then the difference in the gap size between these two HTS's needs another explanation. It is possible, due to the strength of the interplane bonding, that the tunneling measurement is probing predominantly the surface of the Tl-2201 crystals which has been exposed to air and may have properties different from the bulk. This raises the possibility that the surface of Tl-2201 may be slightly overdoped, which results in a smaller gap size. When Bi-2212 is annealed in air it has a $T_c \sim 86$ K and is slightly overdoped. This is the equilibrium oxygen doping level at atmospheric conditions and a similar situation is found for Tl-2201. Air annealed Tl-2201 has a $T_c \sim 82$ K. Therefore, air-exposed Tl-2201 will have a tendency for the surface to be somewhat overdoped by coming to equilibrium with atmospheric conditions. We are then suggesting that when the sample is cooled down to 4.2 K, there are no changes in the surface concentration. Of course we have no proof of this. If there are changes in the surface concentrations upon cooling in vacuum, then these changes are highly reproducible because both Bi-2212 and Tl-2201 display highly reproducible spectra and gap values.

Furthermore, the strength of the dip feature seems to indicate that the surface is slightly overdoped. In Bi-2212, tunneling conductances exhibiting gap sizes of 35-40 meV exhibit dip strength of approximately 80% of the background conductance. For smaller gaps in the range of 15-20 meV (which are from overdoped Bi-2212), the dip strength is approximately 10%. [1] This is consistent with what is observed in Fig. 5 for Tl-2201 and seems to support our argument that the surface of Tl-2201 crystals we measured is slightly overdoped. This however, is still speculation and requires further detailed study to account for the apparent gap size discrepancy. We note that preliminary temperature dependent data indicate that junctions which exhibit small gaps (~ 20 meV) also show a strong smearing out of the gap feature at a temperature below the bulk T_c .

To summarize, we have performed SIN tunneling junction measurements on single crystals of Tl-2201 with bulk T_c of 86 K. The conductance data obtained reproducibly show cusp-like subgap features, asymmetric conductance peaks and weakly decreasing backgrounds. These observations are consistent with our earlier report on Tl-2201 with a T_c of 91 K that were synthesized in a different manner. The present data are fit reasonably well with two different models using the d -wave gap symmetry. The need for a weighting function in Model I and the prominent asymmetry of the data which is reproduced in Model II seem to indicate that the tunneling process in these cases may have a weak preferential tunneling direction centered at or near the absolute maximum of the d -wave gap. The magnitude of the superconducting gap for this cuprate is noticeably smaller than the gap size of optimally-doped Bi-2212 that has similar T_c . The existence of a universal relationship between the superconducting gap size and T_c is still undetermined, and therefore the origin of the discrepancy between the gap size of these two cuprates is still uncertain.

V. ACKNOWLEDGMENTS

This work was partially supported by U.S. Department of Energy, Division of Basic Energy Sciences-Material Sciences under contract No. W-31-109-ENG-38, and the National Science Foundation, Office of Science and Technology Centers under contract No. DMR 91-20000. Z.Y. acknowledges support from the Division of Educational Programs, Argonne National Laboratory.

- [1] Y. DeWilde, N. Miyakawa, P. Guptasarma, M. Iavarone, L. Ozyuzer, J. F. Zasadzinski, P. Romano, D. G. Hinks, C. Kendziora, G. W. Crabtree and K. E. Gray, *Phys. Rev. Lett.* **80**, 153 (1998).
- [2] C. Renner, O. Fisher, *Phys. Rev. B* **51**, 9208 (1995).
- [3] P. Romano, J. Chen, J. F. Zasadzinski, *Physica C* **295**, 15 (1998).
- [4] J. Chen, J. F. Zasadzinski, K. E. Gray, J. L. Wagner, D. G. Hinks, *Phys. Rev. B* **49**, 3683 (1994).
- [5] J. Y. T. Wei, C. C. Tsuei, P. J. M. van Bentum, Q. Xiong, C. W. Chu, M. K. Wu, *Phys. Rev. B* **57**, 3650 (1998).
- [6] M. Covington, M. Aprili, E. Paraoanu, L. H. Greene, F. Xu, J. Zhu, C. A. Mirkin, *Phys. Rev. Lett.* **79**, 277 (1997).
- [7] J. Y. T. Wei, N.-C. Yeh, D. F. Garrigus, and M. Strasik, *Phys. Rev. Lett.* **81**, 2542 (1998).
- [8] S. Sinha and K. -W. Ng, *Phys. Rev. Lett.* **80**, 1296 (1998).
- [9] J. R. Kirtley, C. C. Tsuei, J. Z. Sun, C. C. Chi, L. S. Yu-Jahnes, A. Gupta, M. Rupp, and M. B. Ketchen, *Nature* **373**, 225 (1995).
- [10] K. A. Kouznetsov, A. G. Sun, B. Chen, A. S. Katz, S. R. Bahcall, J. Clarke, R. C. Dynes, D. A. Gajewski, S. H. Han, M. B. Maple, J. Gianpintzakis, J. -T. Kim and D. M. Ginsberg, *Phys. Rev. Lett.* **79**, 3050 (1997).
- [11] Q. Huang, J. F. Zasadzinski, N. Tralshawala, K. E. Gray, D. G. Hinks, J. L. Peng, R. L. Greene, *Nature (London)* **347**, 369 (1990).
- [12] D. H. Wu, J. Mao, S. N. Mao, J. L. Peng, X. X. Xi, T. Venkatesan, R. L. Greene, S. M. Anlage, *Phys. Rev. Lett.* **70**, 85 (1993).
- [13] Z. -X. Shen, D. S. Dessau, B. O. Wells, D. M. King, W. E. Spicer, A. J. Arko, D. Marshall, L. W. Lombardo, A. Kapitulnik, P. Dickinson, S. Doniach, J. DiCarlo, A. G. Loeser and C. H. Park, *Phys. Rev. Lett.* **70**, 1553 (1993).
- [14] G. T. Jeong, J. I. Kye, S. H. Chun, S. Lee, S. I. Lee, and Z. G. Khim, *Phys. Rev. B* **49**, 15416 (1994).
- [15] Z. Yusof, J. F. Zasadzinski, L. Coffey, and N. Miyakawa, *Phys. Rev. B* **58**, 514 (1998).
- [16] C. C. Tsuei, J. R. Kirtley, Z. F. Ren, J. H. Wang, H. Raffy, and Z. Z. Li, *Nature* **387**, 481 (1997).
- [17] M. Willemin, C. Rossel, J. Hofer, H. Keller, Z. F. Ren, J. H. Wang, *Phys. Rev. B* **57**, 6137 (1998).
- [18] L. Ozyuzer, Z. Yusof, J. F. Zasadzinski, R. Mogilevsky, D. G. Hinks, K. E. Gray, *Phys. Rev. B* **57**, 3245 (1998).
- [19] C. Storm, S. G. Ericsson, L. G. Johansson, A. Simon, H. J. Mattausch, R. K. Kremer, *J. Solid State Chem.* **109**, 321 (1994).
- [20] Y. Shimakawa, Y. Kubo, T. Manako, H. Igarashi, *Phys. Rev. B* **40**, 11400 (1989).
- [21] L. Ozyuzer, J. F. Zasadzinski, K. E. Gray, *Cryogenics* **38**, 911 (1998).
- [22] L. Ozyuzer, J. F. Zasadzinski, C. Kendziora, K. E. Gray (unpublished).
- [23] C. Manabe, M. Oda, and M. Ido, *J. Phys. Soc. Jap.* **66**, 1776 (1997).
- [24] H. Won and K. Maki, *Phys. Rev. B* **49**, 1397 (1994).
- [25] M. Ledvij, R. A. Klemm, *Phys. Rev. B* **51**, 3269 (1995).
- [26] M. R. Norman, M. Randeria, H. Ding, J. C. Campuzano, *Phys. Rev. B* **52**, 615 (1995).
- [27] D. J. Singh, W. E. Pickett, *Physics C* **203**, 193 (1992).
- [28] W. A. Harrison, *Phys. Rev.* **123**, 85 (1961).
- [29] J. F. Zasadzinski, L. Ozyuzer, Z. Yusof, J. Chen, K. E. Gray, R. Mogilevsky, D. G. Hinks, J. L. Cobb, J. T. Market, *Spectroscopic Studies of High Tc Cuprates*, ed. I. Bozovic, D. van der Marel, *Proc. SPIE* **2696**, 338 (1996) (Bellingham).

Fig. 1. Tunneling conductances of eight junctions on three different Tl-2201 crystals, each with a bulk T_c near 86 K. Junction A, B, C, E, and F have been shifted vertically by 1.5, 1.2, 0.7, 0.3, and 0.1 mS respectively for clarity in their own scales.

Fig. 2. (a) SIN tunneling conductance of Junction E (circles) at 4.2 K and the estimated normal state conductance (line). (b) Comparison of the normalized SIN conductance with Model I. The inset shows the angular weighting function $f(\theta)$. (c) Comparison of the unnormalized conductance with Model II. Refer to Ref. [15] for definitions of variables. c_o , which corresponds to the chemical potential, has been changed to 0.1585 eV for all comparisons done in this paper.

Fig. 3. (a) SIN tunneling conductance of Junction J (circles) at 4.2 K and the estimated normal state conductance (line). (b) Comparison of the normalized SIN conductance with Model I. (c) Comparison of the unnormalized conductance with Model II.

Fig. 4. (a) SIN tunneling conductance of Junction B' (circles) at 4.2 K and the estimated normal state conductance (line). (b) Comparison of the normalized SIN conductance with Model I. (c) Comparison of the normalized SIN conductance of Junction C' with Model I. The tunneling conductance has been normalized by a constant.

Fig. 5. SIS conductance curves generated from the unnormalized SIN conductance curves of Junction E and B'. Each SIS curve shows the prominent dip feature at nearly 3Δ .

Fig. 1 Ozyuzer et al.

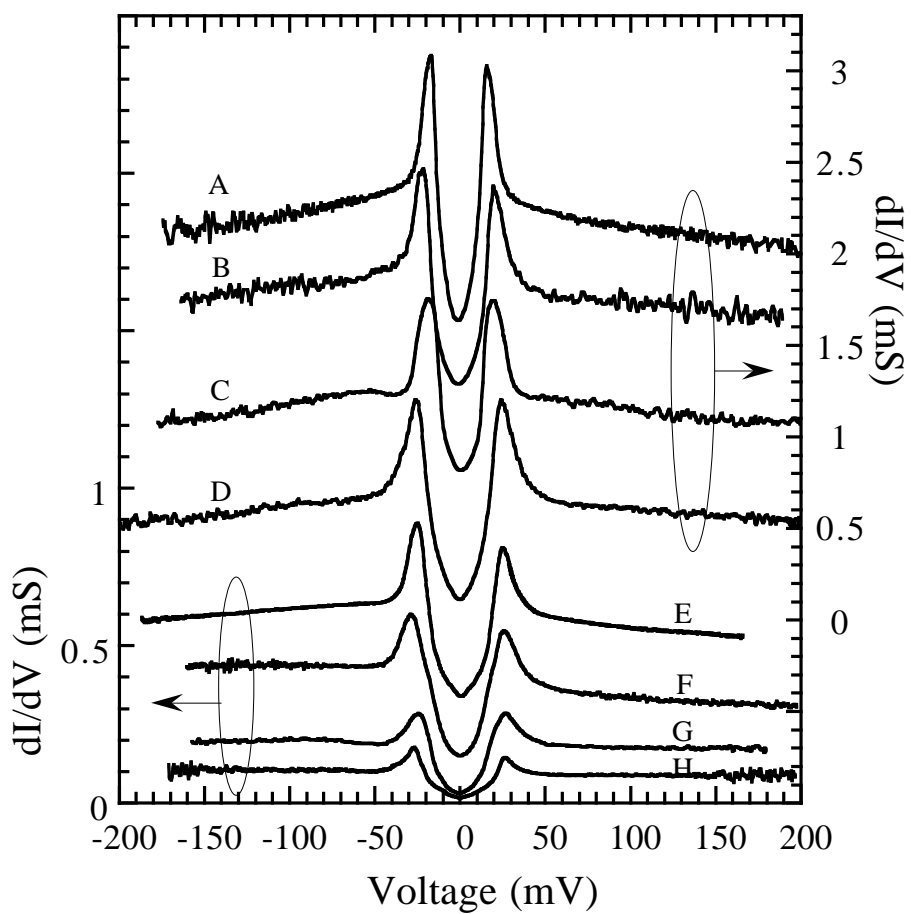


Fig. 2(a) Ozyuzer et al.

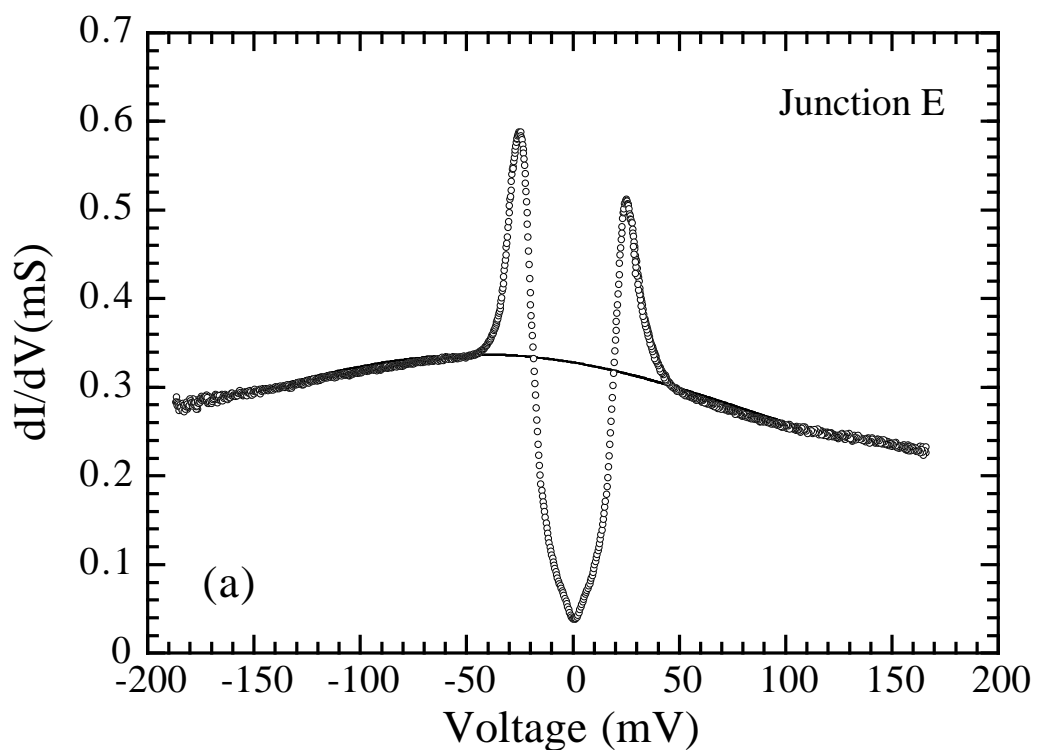


Fig. 2(b) Ozyuzer et al.

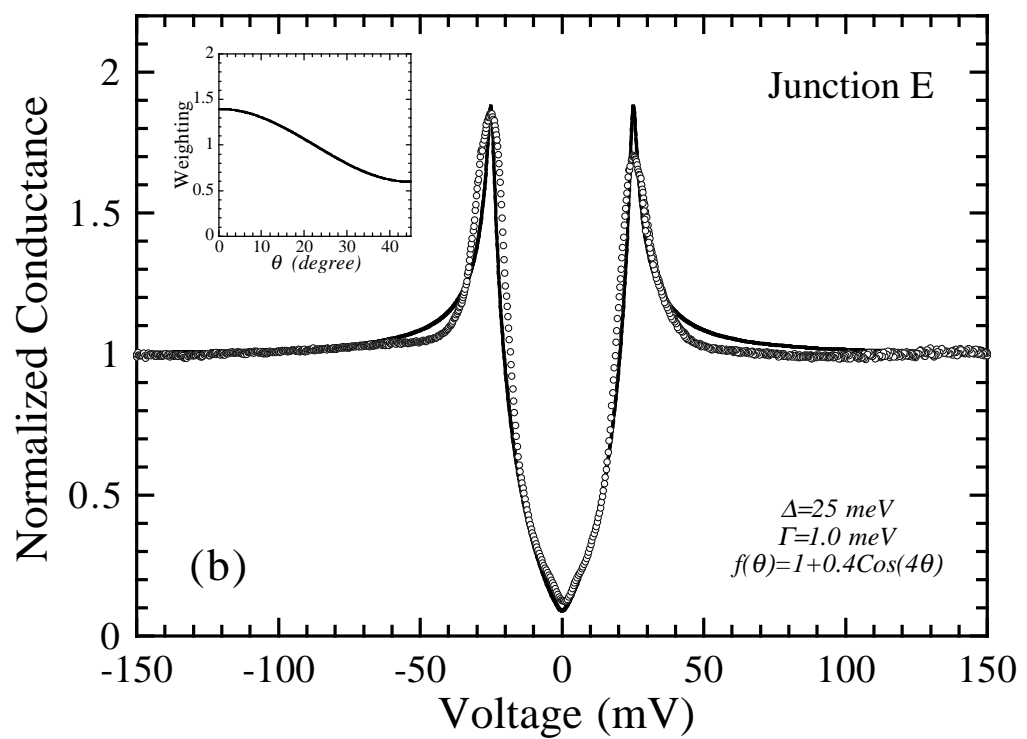


Fig. 2(c) Ozyuzer et al.

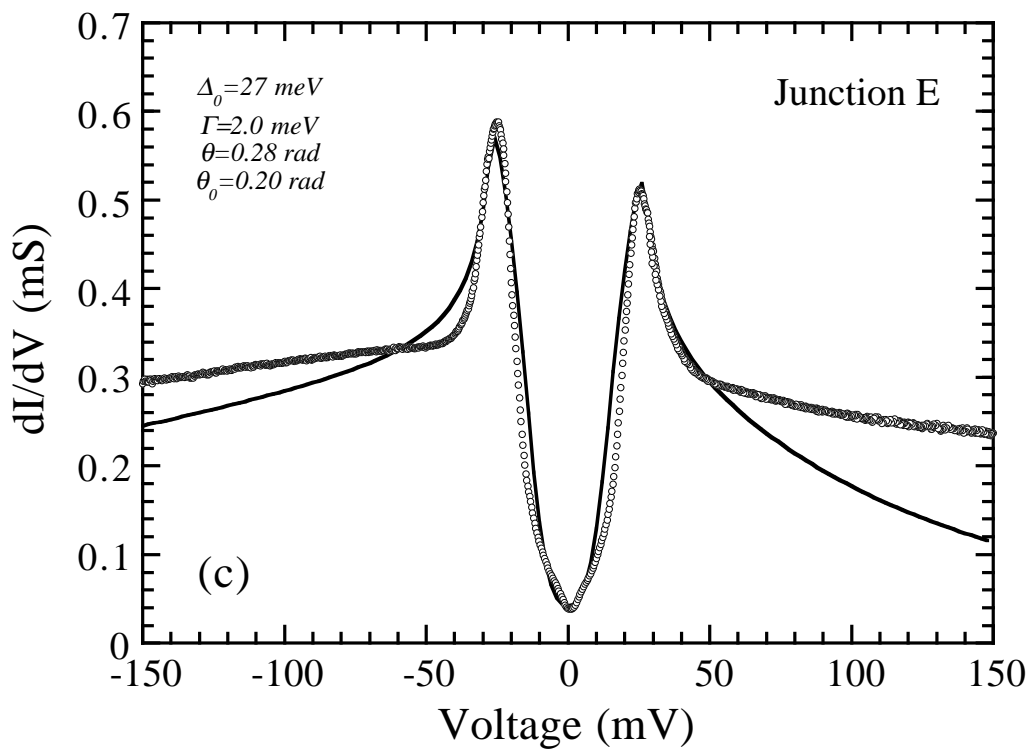


Fig. 3(a) Ozyuzer et al.

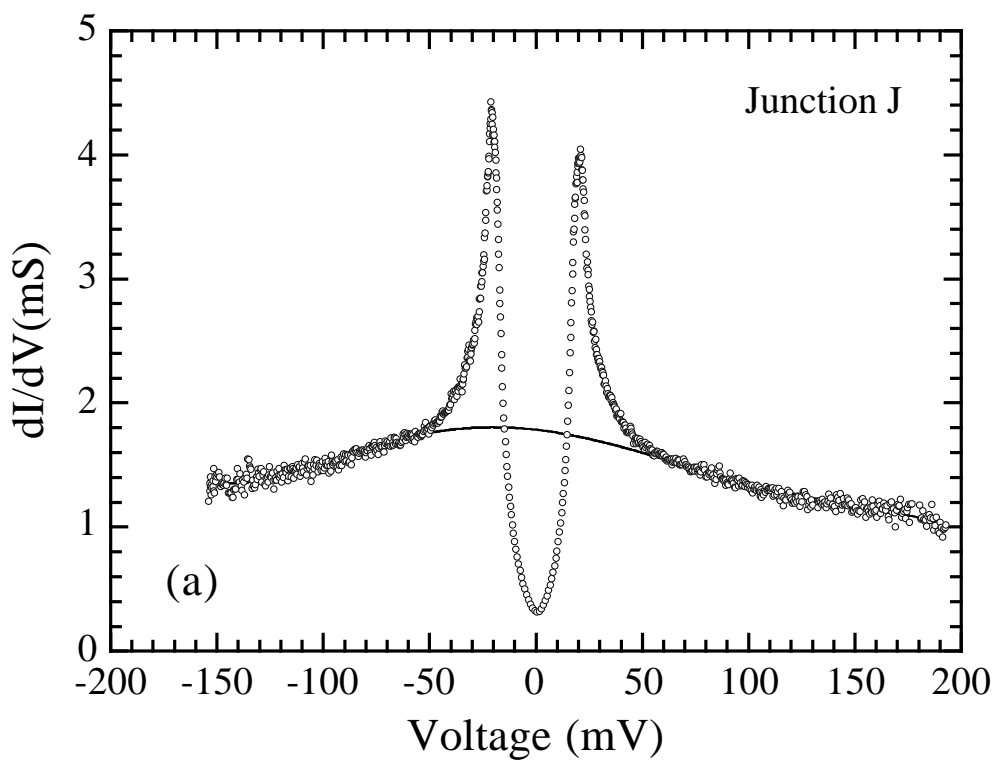


Fig. 3(b) Ozyuzer et al.

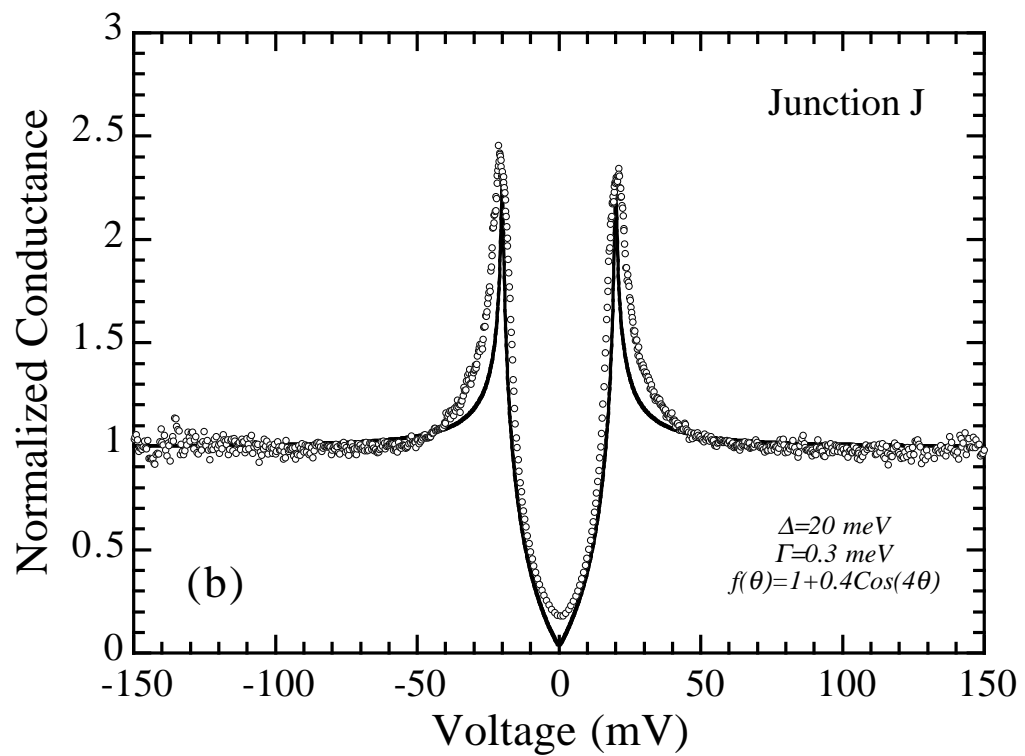


Fig. 3(c) Ozyuzer et al.

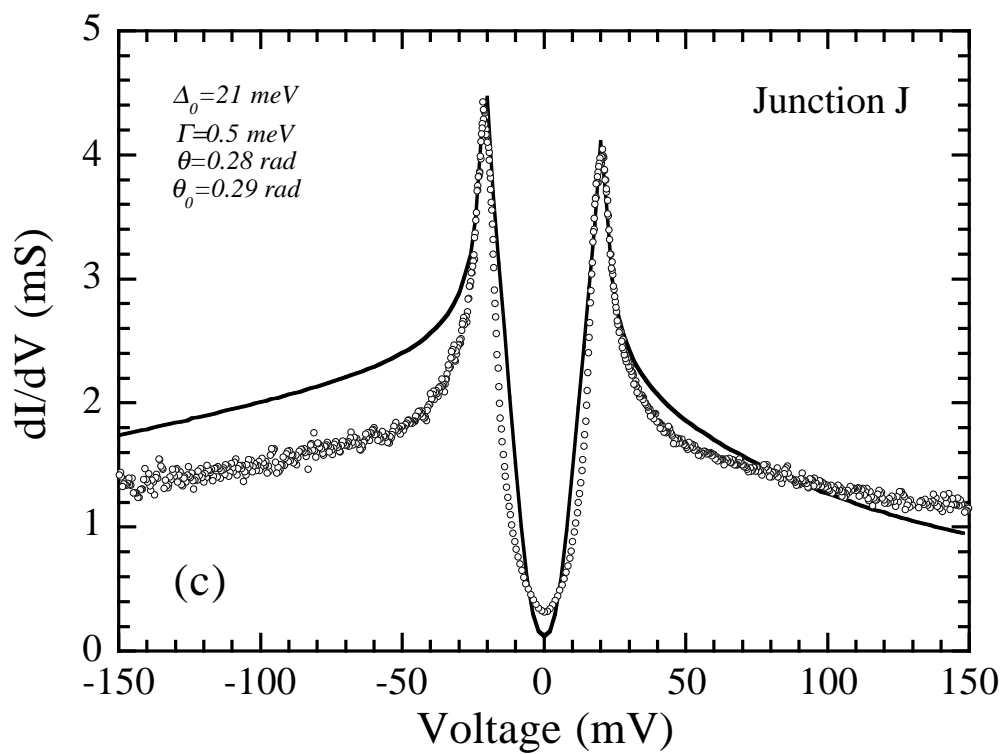


Fig. 4(a) Ozyuzer et al.

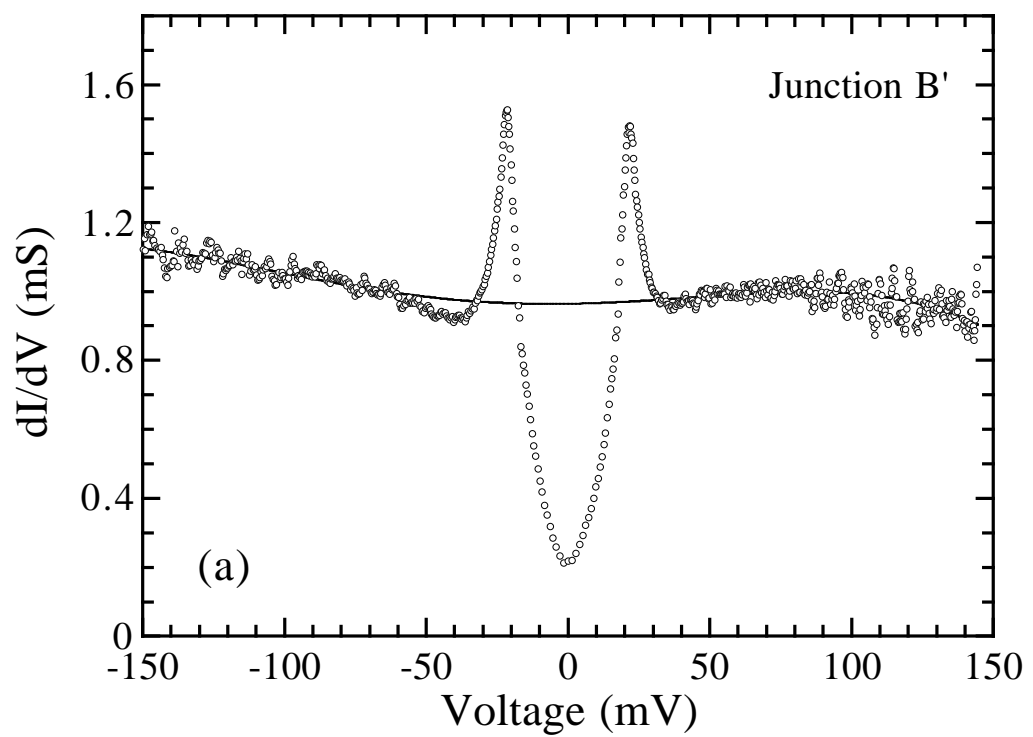


Fig. 4(b) Ozyuzer et al.

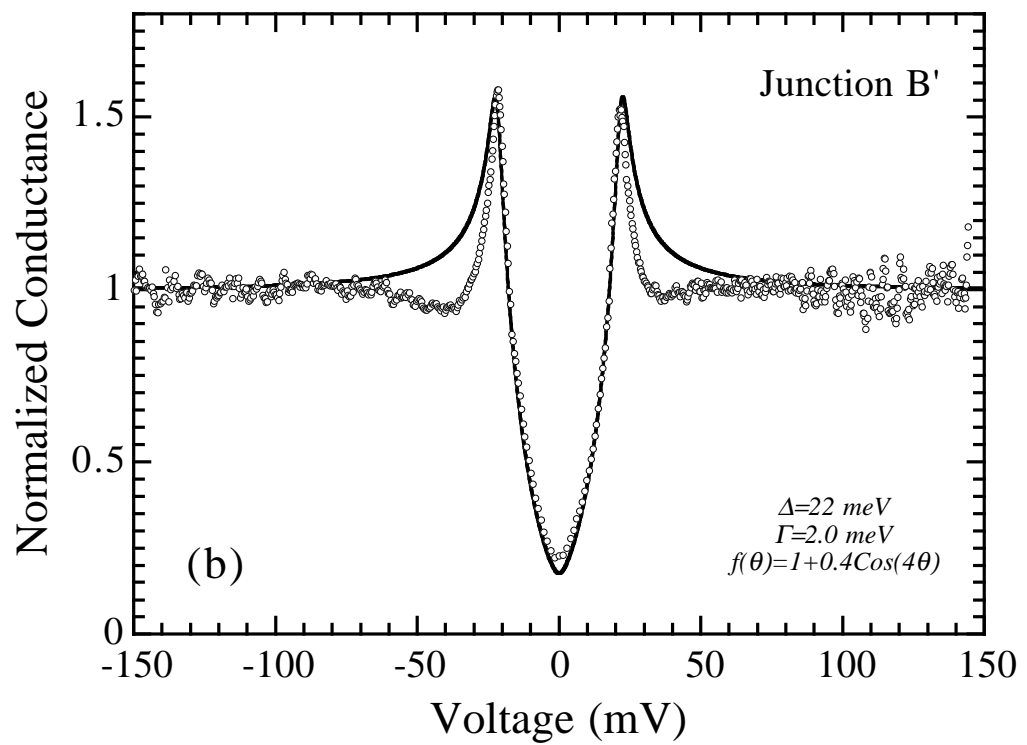


Fig. 4(c) Ozyuzer et al.

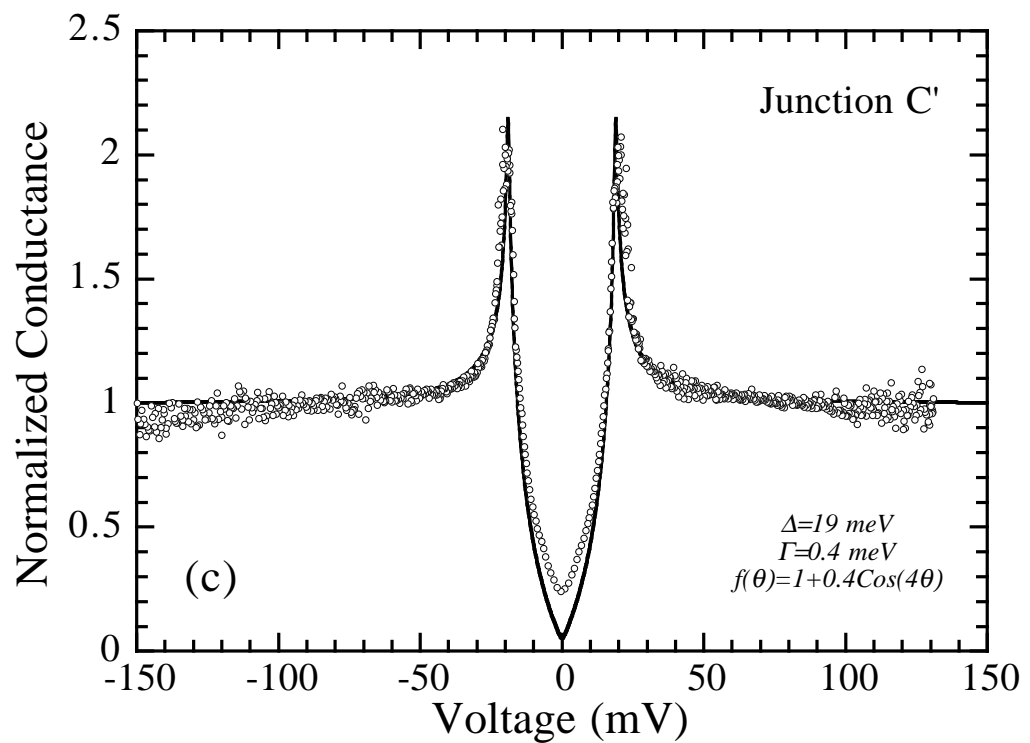


Fig. 5 Ozyuzer et al.

